ARL-TR-8189 ● OCT 2017

US Army Research Laboratory

Design of Alpha-Voltaic Power Source Using Americium-241 (^{241}Am) and Diamond with a Power Density of 10 mW/cm^3

by John Langley, Marc Litz, Johnny Russo, and William Ray Jr

Approved for public release; distribution is unlimited.

NOTICES

Disclaimers

The findings in this report are not to be construed as an official Department of the Army position unless so designated by other authorized documents.

Citation of manufacturer's or trade names does not constitute an official endorsement or approval of the use thereof.

Destroy this report when it is no longer needed. Do not return it to the originator.

ARL-TR-8189 ● OCT 2017

US Army Research Laboratory

Design of Alpha-Voltaic Power Source Using Americium-241 (^{241}Am) and Diamond with a Power Density of 10 mW/cm^3

by John Langley, Marc Litz, and Johnny Russo
Sensors and Electron Devices Directorate, ARL

William Ray Jr
Oak Ridge Associated Universities Journeyman Program,
Oak Ridge, Tennessee

Approved for public release; distribution is unlimited.

REPORT DOCUMENTATION PAGE

Form Approved
OMB No. 0704-0188

Public reporting burden for this collection of information is estimated to average 1 hour per response, including the time for reviewing instructions, searching existing data sources, gathering and maintaining the data needed, and completing and reviewing the collection information. Send comments regarding this burden estimate or any other aspect of this collection of information, including suggestions for reducing the burden, to Department of Defense, Washington Headquarters Services, Directorate for Information Operations and Reports (0704-0188), 1215 Jefferson Davis Highway, Suite 1204, Arlington, VA 22202-4302. Respondents should be aware that notwithstanding any other provision of law, no person shall be subject to any penalty for failing to comply with a collection of information if it does not display a currently valid OMB control number.
PLEASE DO NOT RETURN YOUR FORM TO THE ABOVE ADDRESS.

1. REPORT DATE *(DD-MM-YYYY)*	2. REPORT TYPE	3. DATES COVERED (From - To)
October 2017	Technical Report	19 June 2017–25 August 2017

4. TITLE AND SUBTITLE

Design of Alpha-Voltaic Power Source Using Americium-241 (^{241}Am) and Diamond with a Power Density of 10 mW/cm^3

5a. CONTRACT NUMBER

5b. GRANT NUMBER

5c. PROGRAM ELEMENT NUMBER

6. AUTHOR(S)

John Langley, Marc Litz, Johnny Russo, and William Ray Jr

5d. PROJECT NUMBER

5e. TASK NUMBER

5f. WORK UNIT NUMBER

7. PERFORMING ORGANIZATION NAME(S) AND ADDRESS(ES)

US Army Research Laboratory
Sensors and Electron Devices Directorate (ATTN: RDRL-SED-E)
2800 Powder Mill Road
Adelphi, MD 20783-1138

8. PERFORMING ORGANIZATION REPORT NUMBER

ARL-TR-8189

9. SPONSORING/MONITORING AGENCY NAME(S) AND ADDRESS(ES)

10. SPONSOR/MONITOR'S ACRONYM(S)

11. SPONSOR/MONITOR'S REPORT NUMBER(S)

12. DISTRIBUTION/AVAILABILITY STATEMENT

Approved for public release; distribution is unlimited.

13. SUPPLEMENTARY NOTES

14. ABSTRACT

Long-lived isotope power sources can provide remotely located sensors and communications nodes with decades of power. Beta-voltaic power sources have been developed for the nanowatt and microwatt power levels. The use of alpha emitters (alpha–voltaics) would increase the energy output by a factor of 100 using the same size, weight, and packaging. Wide band-gap radiation-tolerant semiconductors (diamond, gallium nitride, and silicon carbide) are evaluated in order to convert the 5-MeV alpha decays into electrical current. Alpha energy deposition in diamond and gallium nitride (GaN) was calculated and compared. Alpha-voltaic energy converters were designed in diamond and GaN based on the energy deposition calculations. Diamond p+/p– structures of 9-μm thickness each would place the depletion region at the maximum energy deposition location. The device structures are described.

15. SUBJECT TERMS

isotope power source, direct energy conversion, diamond energy converter, alpha-voltaic, long-lived sensor power supply

16. SECURITY CLASSIFICATION OF:			17. LIMITATION OF ABSTRACT	18. NUMBER OF PAGES	19a. NAME OF RESPONSIBLE PERSON
a. REPORT	b. ABSTRACT	c. THIS PAGE			Marc Litz
Unclassified	Unclassified	Unclassified	UU	38	19b. TELEPHONE NUMBER (Include area code) (301) 394-5556

Standard Form 298 (Rev. 8/98)
Prescribed by ANSI Std. Z39.18

Contents

Approved for public release; distribution is unlimited.

List of Figures

List of Tables

1. Introduction

The US Army's status as the most technologically advanced fighting force in the world is achieved by making the most out of what is generally available. Americium-241 ([^{241}Am], the isotope in smoke detectors) is one of the most widely available and affordable sources of alpha radiation. ^{241}Am has a half-life of 432 years, enabling long-lived power and high energy density for sensors and communications devices located in remote or harsh environments. The regulations for shipping and handling ^{241}Am are well documented and understood. In addition, the activity levels that meet all of the Nuclear Regulatory Commission and Department of Transportation regulations are large enough that it is practical to develop a 10 mW/cm^3 power source and handle units logistically through commercial transport.[1] We then designed an energy converter using ^{241}Am in a diamond p–/p+ diode that achieved 10 mW/cm^3.

The US Army needs a power source for applications that addresses the need for battlefield awareness, ubiquitous sensing in remote locations, and DARPA's Internet of Things low-draw sensor networks that increase soldier survivability through omnipresent threat-detection capabilities. These sensors need to be powered for decades with high enough energy densities for scalability. Alpha-voltaic energy converters provide higher energy densities than any other power source. Figure 1 is a Ragone plot[2] with energy density plotted against power density and output time. "A" and "B" on the chart refer respectively to a 100-μW beta-photovoltaic (BPV) that was developed and a 10-mW BPV that is currently being developed.

The Ragone plot shows that alpha decay energy density is 3 orders of magnitude greater than most beta decaying isotopes. It is expected that alpha-voltaics can be designed to have greater than 100 times more output energy than beta-voltaics assuming a 10% conversion efficiency. With a shorter range, α radiation with energies under 10 MeV also avoid complicated scattering occurring with β interactions.[3] One consequence of the pursuit of a much higher energy radioisotope is that its radiation damage to the energy conversion material must be investigated; the radiation damage from 5-MeV α particles is greater than from the 20-keV β particles commonly used in beta-voltaics and BPVs.

Approved for public release; distribution is unlimited.

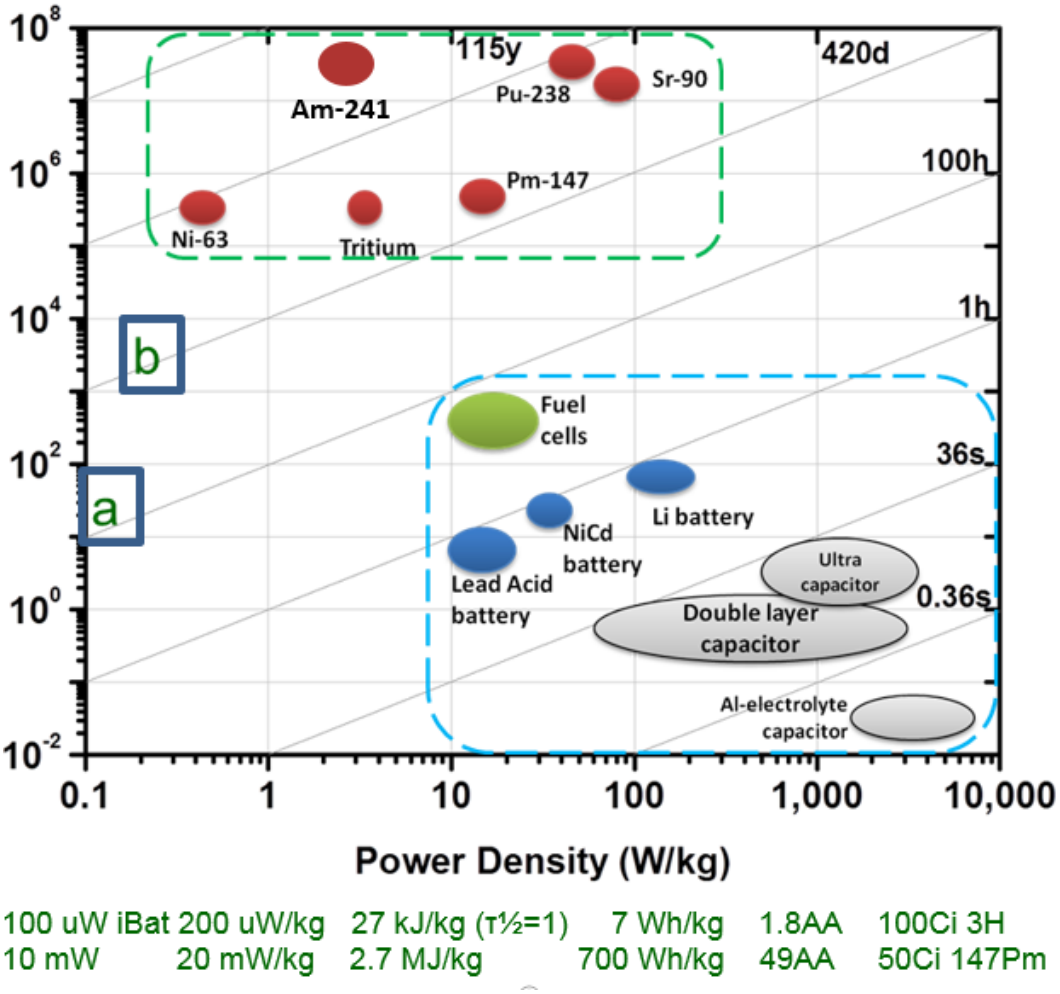

Fig. 1 Alpha isotopes provide increased energy density over existing beta-voltaics

1.1 State of Art of Diamond Electronic Devices

Research into diamond growth and device manufacturability is not up to par with current knowledge of silicon, gallium nitride, etc. devices. Interest in diamond is being generated due to diamond's wide band-gap, small lattice constant, radiation hardness, high carrier mobility, and low leakage current among other factors. Other wide band-gap materials have also demonstrated considerable radiation tolerance. It is known, for example, that gallium nitride (GaN) can take at least 2 orders of magnitude more dose than the maximum doses in gallium arsenide (GaAs).[4]

Work has been done to determine diamond semiconductor characteristics such as Schottky contact material, charge collection efficiency (CCE), and device degradation. Some examples of this work include Tarelkin et al.[5] who found that, for low-energy electrons, all popular configurations of Schottky regions demonstrated at least 90% electron-hole pair (EHP) collection. This study also

correlated higher efficiencies with higher radiation energy, reaching near 100% collection efficiency.[5] Another study determined the theoretical maximum efficiency of a silicon carbide alpha-voltaics energy converter to be 3.6%. It stated that alpha-voltaics have a higher maximum efficiency than beta-voltaics because alpha energy deposition scales well with all energy converter dimensions.[6]

1.2 Energy Conversion Devices

Previous research with energy conversion devices has led to multiple insights for the optimization of output power efficiency, power density, and device configuration. Michigan State University (MSU) designed several diamond energy converters in vertical and pseudo-vertical configurations.[7] Pseudo-vertical, or quasi-vertical, configurations consist of active semiconductor layers grown vertically differing from vertical devices with the placement of both metal contacts on the top side of each layer. MSU's diamond energy converters used p–/p+ boron doping with a Schottky contact. Kone et al.[8] modeled and developed a p-type diamond Schottky diode quasi-vertical device citing the lack of efficiency of n-type doping in diamond. The demonstrated device shown in Fig. 2 came with predicted outputs of 1 200 A/cm^2, but found evidence pointing to an excess of defects in the bulk. It was suggested to improve the device by increasing the p– layer. Kone's team still awaits more precise measurements to match the modeling predictions.[8]

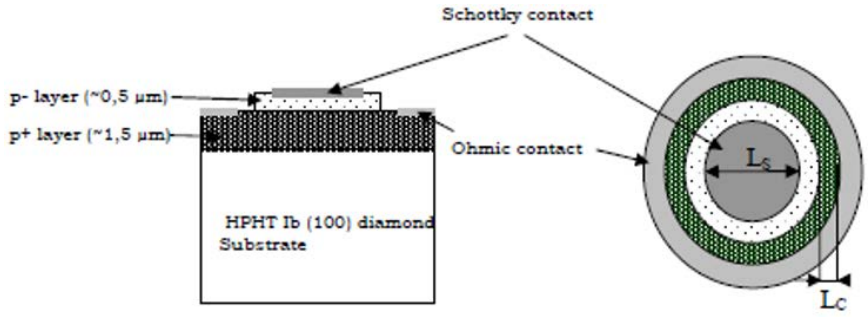

Fig. 2 Schottky barrier diode (Kone et al.)[8]

Bormashov et al.[9] fabricated a Schottky barrier diamond diode that achieved 120 W·hr/kg with a ^{63}Ni beta source, but they only achieved a total efficiency of 0.6%. When they applied a ^{238}Pu α source they achieved their maximum output power of 2.4 µW/cm^2 before measuring a 50% power loss after 10 hours. To remedy this, Bormashov suggested optimizing the diode dimensions to stop the alphas in non-active substrate layer; the damage to the device occurs at the end of the α range.

Various researchers have approached the α-based isotope energy converter challenge by employing α-photovoltaics. In α-photovoltaics, the ionizing radiation interacts with a phosphor to release photons. Then, solar cells capture the photons

and convert them into an electrical current. A ^{238}Pu α-photovoltaic power source was developed using AlGaAs that achieved an 11% efficiency and a 21-μW power output.[10] The device only lost 19% of its radioluminescence from a dose of 26.3(10^7) J/kg corresponding to 411 h of continuous operation.

Other efforts in energy conversion were conducted by Cress et al.[11] and Prelas et al.[12] Cress et al. extended the lifetime of an InGaP α-voltaic energy converter 10 times by growing an intrinsic layer in which the alphas were deposited.[11] They achieved 36.3% CCE with 0.141 mCi/cm^2 α decaying isotope. Prelas et al. predicted 44.2% of ionization energy going to EHP production and a 0.3% maximum efficiency of diamond Schottky barrier energy converters. Prelas et al. said that the limiting factors to nuclear batteries were getting a good match between the range of the ionizing radiation in the material and the dimensions of the energy converter and optimizing depletion region width.[12]

1.3 Isotope Availability and Safety

Select α-emitting isotopes used in energy conversion devices are available and ubiquitous. Isotopes that decay by α emission are used in a variety of industrial applications. Pacemaker batteries made with plutonium-238, radon-226, palladium-103, and cesium-131 are used in cancer treatments,[13] and ^{241}Am is used in smoke detectors.

Smoke detectors are a very productive use of radiation in our homes. Americium-241 α particles ionize the air between 2 charged plates, completing a circuit. Smoke particles enter the ionization chamber and drop the current, which triggers an alarm. This process is going on across the globe safely due to the short range and lack of penetration from alpha particles.[14] Alphas propagate in air only approximately 4 cm and only up to approximately 50 μm in human tissue. While they are dangerous if ingested, alpha particles cannot penetrate human skin.

2. Background of Alpha Interaction with Matter

Using a diamond wide band-gap semiconductor, alpha-voltaic batteries hurtle contemporary power-weight ratio limitations and provide a long-term solution for low-energy applications. Radiation (e.g., with α's) affects the power source's life and conversion efficiency. Alpha particles are a heavy, doubly charged energetic particle given off by isotopes to become more stable. With their double charge, alphas interact primarily with electrons and stop at well-defined locations. After transferring their energy to freeing electrons, alpha particles slow down enough to bond with 2 electrons and become the neutral element helium.[15]

2.1 Alpha Energy Loss

There has been research dealing with semiconductor radiation hardening for the space environment, a cosmic cocktail of high-energy radiation.[16] The magnetosphere contains 85% protons, 14% α particles, and 1% heavy ions radiating in isotropic form. The van Allen belts consist of an inner belt of protons up to 600 MeV and an outer belt of electrons.[4] However, due to the earth's magnetic and atmospheric shielding, US Army terrestrial sensors using radioisotope batteries would not be subjected to the high levels of radiation found in space. There is not as much work on the damage effects of terrestrial, low-energy, long-term radiation.

Ions are stopped in materials in 2 ways; ionizing and nonionizing energy loss (NIEL) to the material. For alphas under 10 MeV, stopping power is primarily through electron-screened Coulombic interactions, making for predictable damage calculations.[3] In semiconductor materials, α particles released by ^{241}Am deposit energy through the Coulombic attraction of electrons in the target material (ionization). Giving off ionization energy slows down the alpha and creates energetic electrons, or delta rays. The delta rays have more than enough energy to leave the atom, so they leave and ionize clusters of electrons nearby.[17] Through ionization, α's impart 99.8% of their energy to diamond and GaN (as shown in Fig. 3). The alphas release the last 0.2% of their energy in phonons as NIEL.

NIEL occurs when an α particle or a displaced atom collides with a lattice atom. Either collision will impart all or some of its energy to the target atom. If this energy imparted (E_0) is equal to or greater than the lattice displacement energy (E_d) (i.e., if $E_0 \geq E_d$), then the atom is displaced and the lattice binding energy goes into photon creation. Otherwise, if E_0 is less than E_d, the target atom vibrates in place and sends a wave through the lattice. This wave is known as a phonon.[18]

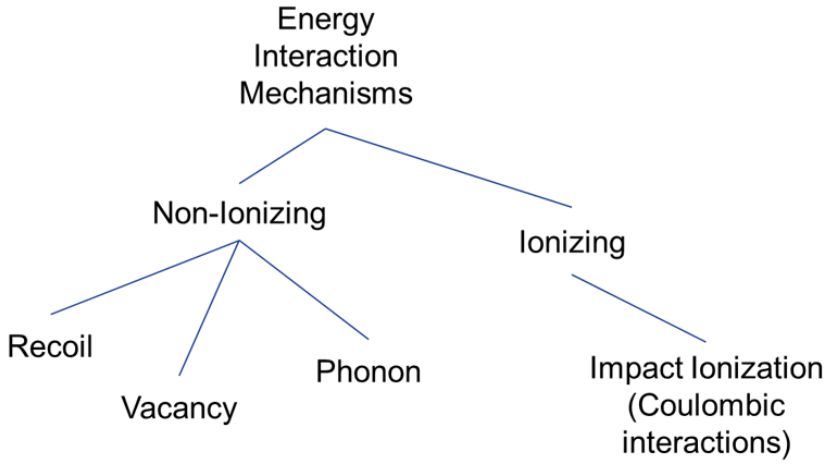

Fig. 3 Alpha interactions with matter are divided into ionizing (99.8%) and nonionizing (0.2%) events for α on diamond

2.2 Materials Damage

Ionizing energy promotes electrons to the conduction band of semiconductors and does not damage the material. NIEL, however, causes damage to the material's lattice structure. NIEL consists of Coulombic elastic, nuclear elastic, and nuclear inelastic interactions that have primary knock-on interactions and produce phonons.[19] These first nuclei to interact leave their place in the lattice and collide with many more nuclei until their energy drops below the lattice displacement energy threshold. At lattice defects sites, the charge carriers (electrons, holes) are trapped and the charge collection efficiency is thus reduced.[20]

Alpha particle NIEL damage mechanisms are vacancy creation, displacements, and creation of phonons in the target. Vacancies are empty locations in ordered lattice structures causing inward relaxation stress, displacements are atoms displaced in a lattice causing outward relaxation stress, and phonons are vibrations in the lattice that can cause damage or help recombine defects. Frenkel pairs are formed by an interstitial leaving its lattice location and leaving a corresponding vacancy.[21]

Linear energy transfer (LET) by ionizing radiation is equivalent to the energy deposition. The LET by ionizing radiation to the material is calculated by

$$\frac{dE}{dx} = \left(\frac{dE}{dx}\right)_{col} + \left(\frac{dE}{dx}\right)_{rad}, \quad (1)$$

where $(dE/dx)_{col}$ is Coulombic interaction energy transfer, and $(dE/dx)_{rad}$ is nuclear interaction energy transfer.[15] Manipulation of SRIM vacancy data and range tables showed most of the nuclear interactions (NIEL damage) occurring at the Bragg peak. The atom displacements plotted alongside recoil energy in diamond and GaN are in Fig. A-1 in Appendix A.

3. SRIM Results

Popular simulation software known as Stopping and Range of Ions in Matter (SRIM) generates energy deposition and collision details for ions in materials. SRIM uses Monte Carlo collision probability distribution functions with empirical data taken across thousands of histories to generate statistically relevant data.

3.1 Trajectory

The trajectories of the first 1,000 particles are shown in Fig. 4. More lateral scattering is shown in the GaN irradiation. This is because of the higher atomic number of gallium compared to carbon in diamond. The end of trajectory (ion range) for the first 1000 particles calculated in the SRIM simulations is shown in

Fig. 5. Because the largest energy deposition (and damage) occurs in the last 2 μm of ion range, the active diode region should end after 10 μm.

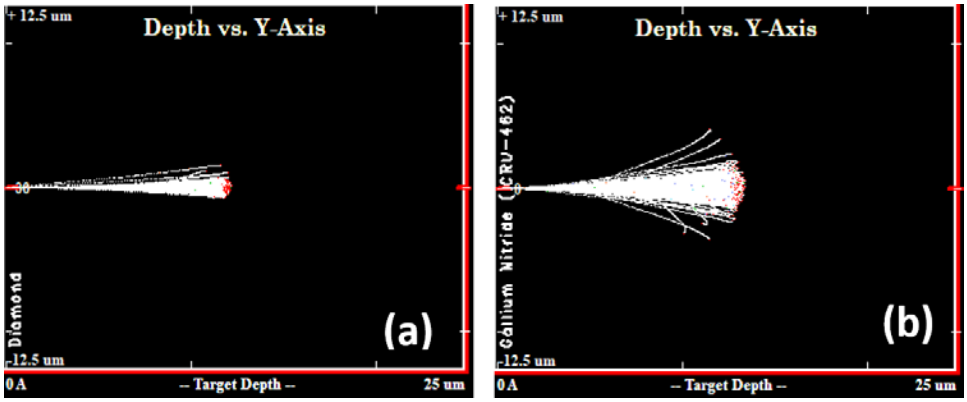

Fig. 4 Ion trajectories in a) diamond and b) GaN

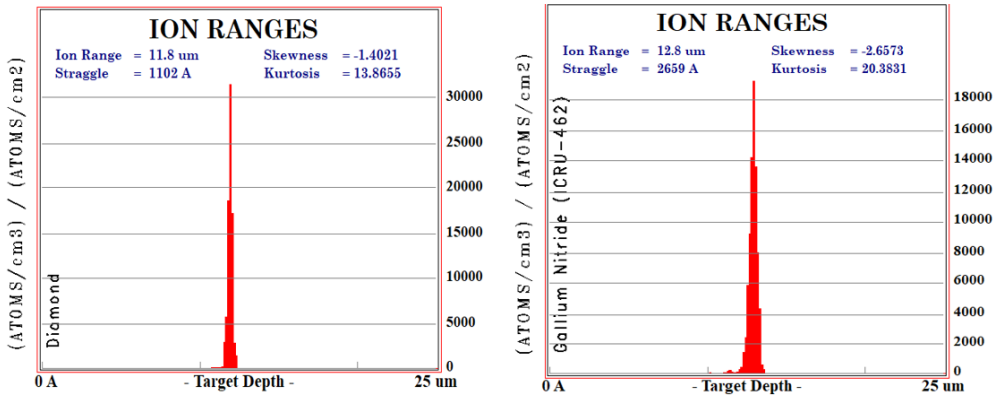

Fig. 5 Ion range distribution in a) diamond and b) GaN. The units are (atoms/cm^3)/(atoms/cm^2). When these plots are multiplied by the fluence in units of (atoms/cm^2) the plot is directly converted to a target density (atoms/cm^3).

SRIM output files with binned data for the number of vacancies and Frenkel Pairs' recombination and the ionizing energy given to each recoil as a function of depth. It also calculates the ion trajectories and distribution in the target. SRIM calculates NIEL effects including displacements, vacancies, interstitials, and replacement collisions. Displacements are calculated as displacements = vacancies + replacement collisions, while vacancies + replacements = interstitials + (atoms which leave the target volume).[18] Collision details were recorded only for collisions that created at least 1 displacement. This fact affected the average number of collisions per ion calculated since, at low energies, the ions collided but had E_0 less than E_d. Although it would have been possible, collision details of the recoil atoms

were not recorded; only primary collision energy loss data was recorded for the collision details data files.

The data in Fig. 6 demonstrate the non-Gaussian final distribution of the ions. The Bragg peak, due to the double charge of the α particles, is where the maximum amount of ionization energy is deposited. The alphas drop below the displacement energy level and quickly absorb electrons to become neutral and settle in a finite region.

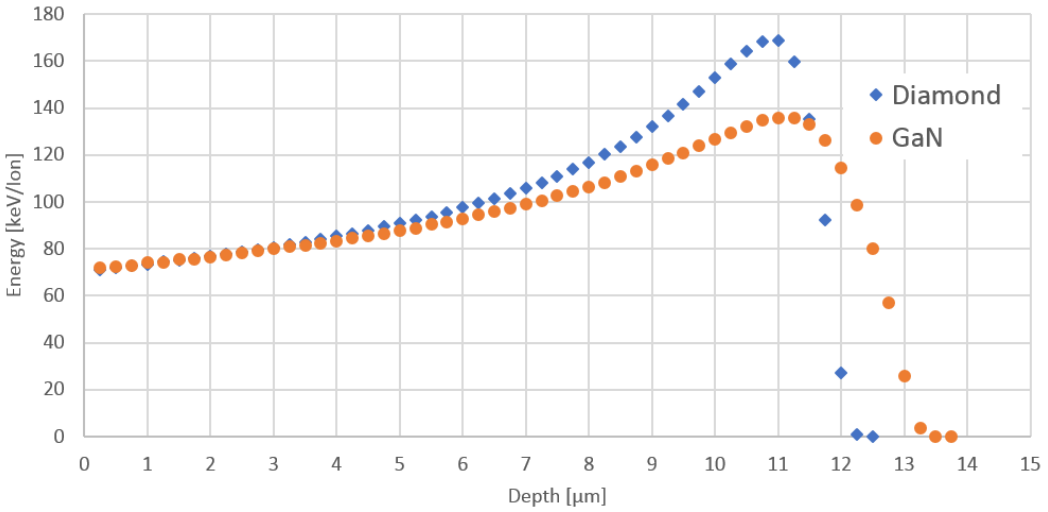

Fig. 6 Alpha particle energy deposition in diamond and GaN. Energy deposition defines optimum location of depletion region.

3.2 Range

The range of the alpha ions calculated by SRIM in diamond and GaN is given in Table 1. The range was 11.8 and 12.8 µm in diamond and GaN, respectively. The ions travel in relatively straight paths, in comparison to electrons, and they are deposited in very close proximity as compared to 5-MeV electron (900 µm range). The range of 5-MeV alphas is much less than 5-MeV betas. Because depletion region in diamond is approximately 1 µm in width, a large fraction of alpha energy goes into EHP production.[12]

Table 1 Range of ion statistics

Ion stopping range table (SRIM)	Target density (g/cm^3)	Ion average range (μm)	Range skewness	Range kurtosis	Ion lateral spread (μm)	Ion radial spread (μm)
Diamond	3.54	11.77	–1.5364	12.9318	0.1530	0.2435
GaN	6.15	12.82	–2.6573	20.3821	0.4554	0.7340
Crystal ZnS	4.09	18.15	–6.8602	139.129	0.6123	0.9626
Powder ZnS	1.50	49.47	–11.8059	273.8109	1.6770	2.6520

Note: Bragg peak is not Gaussian.

3.3 Energy Deposition

SRIM outputs a file of the ionization energy loss in the target material as a function of depth. The energy deposited with respect to depth is binned in units of eV/ion. Multiplying the data by the bin length gave energy per depth. This data was instrumental for determining the optimum location of the depletion region in the semiconductor energy conversion material. The location where half the alpha energy has been deposited is 7.25 μm in diamond (3.5 g/cm^3) and 7.5 μm in GaN (6.1 g/cm^3).

The α particles ionize the semiconductor constituent atoms and create electron-hole pairs (EHPs). The EHPs recombine except at the depletion region, such as a p–/p+ junction, which has an electrical potential. The depletion region is usually up to approximately 1 μm in width. The fraction of ionization energy in these regions versus the range of the particles determines the amount of EHPs collected. Thus, α's, with 12 μm range in diamond, have potential for higher efficiency than β's.[12,6]

SRIM only calculated the α particle collisions that displaced at least 1 atom. The average number of these collisions for α's in diamond was 36 times per individual ion trajectory and was 58 times per ion in GaN. One note in the SRIM manual related that the results are consistent with measurement data at a temperature of 0 K; there are no accommodations for annealing. Annealing at room temperature (300 K) would affect an experiment by assisting in the recombination of defects.

4. Device Design

4.1 Diode Structures for Energy Conversion

Two popular energy converter device configurations are quasi-vertical and vertical devices. A recent study combined the benefits of both while avoiding their pitfalls by making a "corner" architecture device.

4.1.1 Quasi-vertical

Quasi-vertical devices take advantage of the stability and ease of manufacturing given by growing the active diode layers on a thick substrate material. The top active layer is grown in strips on top of the bottom layer, leaving strips of exposed active bottom layer. In the case of diamond Schottky barrier diodes, ohmic contacts are applied to the exposed bottom layer, and Schottky contacts are applied to the top layer.

4.1.2 Vertical

Vertical device structures have both active semiconductor layers sandwiched between the 2 metal contacts. In vertical energy converters, the charge carriers have a shorter distance to travel, and thus higher charge collection efficiency. However, research into vertical devices was stunted by issues of reliably manufacturing the heavily doped, free-standing diamond devices necessary for vertical structures.[22]

4.1.3 Corner Cut

Innovative Schottky barrier diode (SBD) structures using "corner" architecture were designed, grown, and evaluated.[22] The corner device (as shown in Fig. 7) incorporates the efficiency of a vertical current path while avoiding the use of unreliable free-standing p-type doped diamond. The corner design also minimizes the growth of threading dislocations in the epitaxial direction by growing the layers of p– and p+ diamond perpendicular to each other.

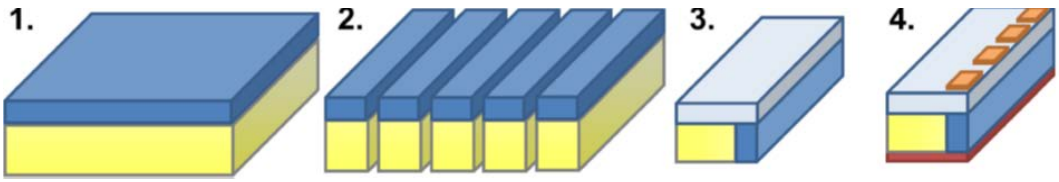

Fig. 7 The growth steps for the fabrication of a corner architecture SBD: 1) Heavily boron-doped diamond is deposited on a type Ib HPHT seed. 2) The sample is then laser-cut lengthwise and both sides of a resulting slab are polished. 3) Lightly boron-doped diamond is grown perpendicular to the direction of the previous CVD growth. 4) Schottky and ohmic contacts are deposited to form a vertically oriented SBD structure.[22]

4.2 Example Power Source

Two example device designs are calculated and compared. A diamond device containing 2 charge collection regions (Schottky and p+/p–) is compared to a GaN (P-i-N) device.

4.2.1 Diamond ^{241}Am

A ^{241}Am powered α direct energy converter in diamond, expected to achieve a power density of 10 mW/cm^3, was proposed. To simplify manufacturing, the proof of concept device would use a quasi-vertical p–/p+ architecture with Schottky and ohmic contacts as shown in Fig. 8. The depletion region was placed at a location depth with optimum energy deposition and collection.

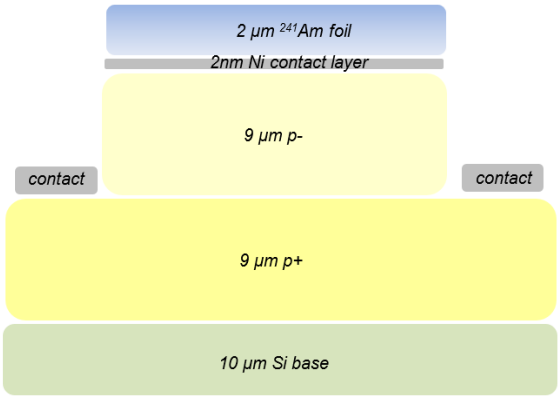

Fig. 8 Quasi-vertical diamond device designed to match energy deposition

4.2.2 Details of Alpha Source Dimensions

The active layers of the energy converter are grown on a substrate of diamond or silicon about 300 μm thick. Nine μm of p+ doped diamond is epitaxially grown on the substrate, and 9 μm of p– diamond is homoepitaxially grown on the previous layer in strips. Ohmic contacts are deposited on the p+ layer between the strips of the top layer, and a Ni Schottky contact is deposited on the top p– layer.

One 1- × 1-cm^2 device had 1 Ci of ^{241}Am deposited over the Schottky contact. The theoretical efficiency of the alpha-voltaic energy converter was calculated. Depletion regions are where an internal electric field exists. Depletion regions were 1-μm thick at the p–/p+ junction (containing 13% of E_{dep} at 10.25 um) and 1 μm at the Schottky barrier (6% of E_{dep}). Total power is characterized as $P_{tot} = A*E_\alpha$ with A being the decay rate of the isotope and E_α being the α particle energy.[6] One Ci of ^{241}Am with a 5 MeV output was converted to total nuclear power:

$$P_{nuc} = 1\ Ci\ * \frac{3.7*10^{10}\frac{decay}{s}}{1\ Ci} * 5\frac{MeV}{decay} * 1.6022 * 10^{-13}\frac{J}{MeV} = 0.0296\ W. \qquad (2)$$

From the equation above 1 Ci of ^{241}Am decay results in output of approximately 30 mW of power. The 5-MeV α range in diamond was numerically calculated to be 11.8 μm. SRIM diamond data (Fig. 6) show that 6% of energy was deposited in the

1-μm region at the Schottky barrier, and 13% of total nuclear kinetic energy from alphas is deposited at the 1-μm region from 10.25 to 11.25 μm.

$$P_{deposited} = 30\,mW * (0.06 + 0.13) = 5.6\,mW. \quad (3)$$

We did not account for electron capture in the diamond or losses in the circuit since diamond has long carrier lifetimes. Thus, the theoretical efficiency of maximum EHP production in diamond is 44.2%.[12] The electrical output power would then be the result of 1) nuclear kinetic energy into the device, 2) the energy deposited in the regions of interest, followed by 3) the charge collection efficiency in the device. A device design encompassing these ideals is illustrated in Fig. 9. The net result, $P_{electrical}$, would be 2.48 mW electrical output from this layered diamond device. Ten 1-cm^2 diamond ^{241}Am devices 1 mm thick each create an ideal power density of 25 mW/cm^3. This power density exceeded our goal of 10 mW/cm^3.

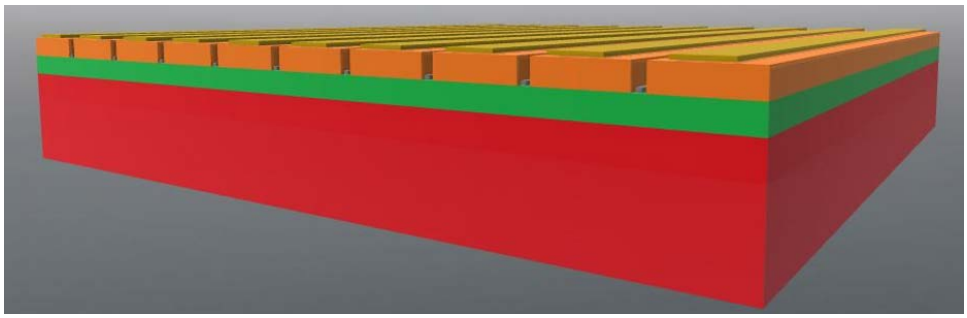

Fig. 9 Three-dimensional quasi-vertical device layout extrapolated from Fig. 8. Built on the bulk diamond base layer (red) is p+ layer (green) and p– layer (orange). Aluminum ohmic contacts are fabricated on top (yellow) as Schottky diode.

The Klein equation suggests 3 to 4 times the band-gap energy is required to create EHPs.[23] Since the diamond band-gap is 5.5 eV, the energy to produce EHPs is E_{EHP} is approximately equal to 19 eV. The SRIM data showed α energy deposition of 660 keV in 1-μm diamond depletion region and 290 keV in 1-μm Schottky region. The rate of EHP production is #EHP = E_{in}/EHP_{avg}, where EHP_{avg} is the average energy required to create an EHPand E_{in} is the energy deposited in the depletion region (units of eV/s). Therefore, the #EHP created in the charge collection regions by α particle from this approach is theoretically as high as 50. In comparison, the numerical calculation from following α particle trajectories in SRIM resulted in 36 EHPs per α particle.

We have previously built GaN beta-voltaic devices.[24] The depletion region was measured using electron beam on 750 nm i-layer GaN device. This represents an alternative design approach to an alpha energy converter using a previously fabricated beta-voltaic device in GaN. The effective electrical power output from alphas can be calculated. The initial nuclear power input from 1 Ci ^{241}Am in the

first 750 nm of GaN is approximately 1.35 mW (reference Fig. 6). If the charge collection efficiency of 30% is used, then the electrical power output expected from a GaN device would be 405 μW, approximately one-sixth of the diamond device.

5. Conclusions

This work describes numerical and analytical calculations toward meeting a goal of 10 mW/cm^3 electrical energy output from an α source. Five MeV α particle ranges are calculated in materials of interest. The availability of ^{241}Am and the energy deposition as a function of depth in diamond allows for flexibility in scaling device charge collection regions to an ionization profile. Consideration for the localized nature of the α radiation NIEL damage near the Bragg peak in diamond would suggest that the active charge collection region should be moved before the Bragg peak in diamond to avoid damage. The Bragg peak, though high-energy deposition, will degrade before the remaining regions.

Future work will determine the electron transport in the energy converter through modeling. SILVACO is an example of a privately owned provider of electron transport modeling in semiconductor materials. This form of computer-aided design will be used to develop and characterize an optimized depletion region width and diffusion lengths from material electrical characteristics. The modeling will aim to match the electric field to the α particle energy deposition for a maximum amount of electron/hole mobility.

The next step will be to fabricate a diamond vertical or quasi-vertical diode and irradiate it. This experiment will give important insights for the future development of alpha-voltaics in the Army. These results will be compared to the modeling data to ensure validity. Additionally, interest in α photovoltaics has recently been aroused. A discussion of recent findings in α photovoltaics is discussed in Appendix B.

6. References

1. US Nuclear Regulatory Commission. Appendix A to part 71—determination of A1 and A2. Rockville (MD): Nuclear Regulatory Commission (US); 2016 July 20 [accessed 2017 Sep 1]. https://www.nrc.gov/reading-rm/doc-collections/cfr/part071/part071-appa.html.

2. Romer MC, Miley GH, Luo N, Gimlin RJ. Ragone plot comparison of radioisotope cells and the direct sodium borohydride/hydrogen peroxide fuel cell with chemical batteries. IEEE Trans Energy Conv. 2008;23(1)171–178.

3. Messenger SR, Burke EA, Summers GP, Walters RJ, Warner JH. Criteria for identifying radiation resistant semiconductor materials. IEEE Trans Nucl Sci. 2005 Dec;52(6):2276–2280.

4. Polyakov A, Pearton S, Frenzer P, Ren F, Liu L, Kim J. Radiation effects in GaN materials and devices. J Mat Chem C. 2013;1(5):877–887.

5. Tarelkin S, Bormashov V, Korostylev E, Troschiev S, Teteruk D, Golovanov A, Volkov A, Kornilov N, Kuznetsov M, Prikhodko D, Buga S. Comparative study of different metals for Schottky barrier diamond betavoltaic power converter by EBIC technique. Physica Status Solidi A. 2016;213(9):2492–2497.

6. Oh K, Prelas M, Lukosi E, Rothenberger J, Schott R, Weaver C, Montenegro D, Wisniewski D. Theoretical maximum efficiency for a linearly graded alphavoltaic nuclear battery. Nucl Tech. 2012;179(2):243–249.

7. Grotjohn TA, Nicley SS, Tran D, Reinhard DK, Becker M, Asmussen J. Single crystal boron-doped diamond synthesis. MRS Proc. 2009;1203.

8. Kone S, Ding H, Schneider H, Isoird K, Civrac G. High performances CVD diamond Schottky barrier diode - simulation and carrying out. Toulouse (France): Université de Toulouse; 2009.

9. Bormashov V, Troschiev S, Volkov A, Tarelkin S, Korostylev E, Golovanov A, Kuznetsov M, Teteruk D, Kornilov N, Terentiev S, et al. Development of nuclear microbattery prototype based on Schottky barrier diamond diodes. Physica Status Solidi A. 2015;212(11):2539–2547.

10. Kavetskiy A, Yakubova G, Yousaf S, Bower K, Robertson JD, Garnov A. Efficiency of Pm-147 direct charge radioisotope battery. App Rad Iso. 2011;69(5):744–748.

11. Cress C, Landi B, Raffaelle R, Wilt D. InGaP alpha voltaic batteries: synthesis, modeling, and radiation tolerance. J App Phys. 2006;100(11):114519.

12. Prelas M, Weaver C, Watermann M, Lukosi E, Schott R, Wisniewski D. A review of nuclear batteries. Prog Nucl Energy. 2014;75:117–148.

13. Mikołajczak R, Bazaniak Z, Iller E. Radioisotopes for medical and industrial use during the 50-year history of the Institute of Nuclear Research. Nukleonika. 2005:83–87.

14. Cleary TG. An analysis of the performance of smoke alarms. Fire Saf Sci. 2001;10:823–836.

15. Holbert KE. Charged particle ionization and range. Lectures from Nuclear Concepts for the 21st Century course. Arizona State University, EEE460-Handout. 2012 Feb 27.

16. NASA Jet Propulsion Laboratory. Alpha-voltaic sources using diamond as conversion medium. Pasadena (CA): NASA Jet Propulsion Laboratory (US); 2006 July. NASA Tech Briefs. p. 33.

17. Knoll GF. Radiation detection and measurement. 3rd ed. Ann Arbor (MI): Wiley; 2000. p. 30–43.

18. Ziegler JF, Biersack JP, Ziegler MD. 9 - TRIM: Output Files. SRIM – the stopping and range of ions in matter. SRIM. Annapolis (MD); 2008. p. 9(1-41).

19. Pearton SJ, Ren F, Patrick E, Law ME, Polyakov AY. Review – ionizing radiation damage effects on GaN devices. ECS J Solid State Sci Tech. 2015 Nov;5(2):Q35–60.

20. Kassel F, Guthoff M, Dabrowski A, de Boer W. Description of radiation damage in diamond sensors using an effective defect model. Physica Status Solidi. 2017.

21. Ashcroft NW, Mermin ND. Solid state physics. Orlando (FL): Harcourt; 1976. p. 620.

22. Nicley S, Zajac S, Rechenburg R, Becker M, Hardy A, Schuelke T, Grotjohn TA. Fabrication and characterization of a corner architecture Schottky barrier diode structure. Physica Status Solidi A. 2015;212(11):2410–2417.

23. Klein CA. Bandgap dependence and related features of radiation ionization energies in semiconductors. J App Phys. 1968 Mar;39(4):2029–38.

24. Khan MR, Smith JR, Tompkins RP, Kelley S, Litz M, Russo J, Leathersich J, Shahedipour-Sandvik F, Jones KA, Iliadis A. Design and characterization of GaN P-i-N diodes for betavoltaic devices. Solid-State Elec. 2017;136:24–29.

25. Bao R, Brand PJ, Chrisey DB. Betavoltaic performance of radiation-hardened high-efficiency Si space solar cells. IEEE Trans Elec Dev. 2012 May;59(5):1286–94.

26. Rybicki G, Vargas-Aburto C, Uribe R. Silicon carbide alphavoltaic battery. 25th Photovoltaic Specialists Conference; 1996; Washington, DC.

27. Bailey SG, Wilt DM, Castro SL, Cress CD, Raffaelle RP. Photovoltaic development for alpha voltaic batteries. IEEE. 2005:106–9.

28. Litz MS, Fan Z, Carroll JJ, Bayne S. Alpha Schottky junction energy source. SPIE; 2012.

29. Summers GP, Burke EA, Shapiro P, Messenger SR, Walters RJ. Damage correlations in semiconductors exposed to gamma, electron, and proton radiations. IEEE Trans Nucl Sci. 1993 Dec;40(6):1372–9.

30. Kong X, Albert S, Bengoechea-Encabo A, Sanchez-Garcia MA, Calleja E, Trampert A. Plasmon excitation in electron energy-loss spectroscopy for determination of indium concentration in (In,Ga)N/GaN nanowires. Nanotechnology. 2012;23(48).

31. Pearton SJ, Deist R, Ren F, Liu L, Polyakov AY, Kim J. Review of radiation damage in GaN-based materials and devices. JVSTA. 2013 Sep.

32. Holbert KE. Radiation effects on materials: displacement damage. Lectures from EE598 Nuclear Concepts for the 21st Century course; 2008 May 16 [accessed 2017 Oct 3]. http://holbert.faculty.asu.edu/eee560/eee560.html.

33. e-Handbook of Statistical Methods. NIST/SEMATECH. 2013 [accessed 2017 July 13]. http://www.itl.nist.gov/div898/handbook/eda/section3/eda35b.htm.

34. Hiraiwa A, Kawarada H. Figure of merit of diamond power devices based on accurately estimated impact ionization processes. J App Phys. 2013 July 21;114(3).

35. Sychov M, Kavetsky A, Yakubova G, Walter G, Yousaf S, Lin Q, Chan D, Socarras H, Bower K. Alpha indirect conversion radioisotope power source. App Rad Iso. 2008;66(2):173–77.

36 Windle WF. Pm147 betavoltaic battery feasibility. Albuquerque (NM): Sandia National Laboratories; 1966.

37. Flicker H, Loferski J, Elleman T. Construction of a promethium-147 atomic battery. IEEE Trans Elec Dev. 1694;11(1):2–8.

38. Loferski JJ, Rappaport P. Radiation damage in Ge and Si detected by carrier lifetime changes: damage thresholds. Phys Rev. 1958;111(2):432–439.

39. Moll M. Radiation damage in silicon detectors. Geneva: Rose Collaboration; 2001.

40. Look DC, Reynolds DC, Hemsky JW, Sizelove JR, Jones RL, Molnar RJ. Defect donor and acceptor in GaN. PRL. 1997;79(12):2273–2276.

41. Ionascut-Nedelcescu, Carlone C, Houdayer A, Bardeleben HV, Cantin JL, Raymond S. Radiation hardness of gallium nitride. IEEE Trans Nucl Sci. 2002;49(6):2733–2738.

42. Kashiwagi T, Hibino K, Kitamura H, Okumo S, Takashima T, Uchihori Y, Yajima K, Yokota M, Yoshida K. Investigation of basic characteristics of synthetic diamond radiation detectors. IEEE Nuclear Science Symposium Conference Record; 2004; Rome, Italy.

43. Ricardo Mori MB. Radiation hardness issues in diamond. Florence: Energetic Department, University of Florence: 2012.

44. Gonon P, Prawer S, Jamieson D, Nugent K. Radiation hardness of polycrystalline diamond. Diamond Relat Mater. 1997;6:314–319.

45. Boer WD, Bol J, Furgeri A, Muller S, Sander C, Berdermann E, Pomorski M, Huhtinen M. Radiation hardness of diamond and silicon sensors compared. Physica Status Solidi (a). 2007;204(9):3004–3010.

46. Trischuk WR. Recent advances in diamond detectors. Toronto, Canada: Department of Physics, University of Toronto; 2008.

INTENTIONALLY LEFT BLANK.

Appendix A. Alpha Particle Cross Section

Some mention should be made of α stopping cross sections. Figures A-1 and A-2 show the effect that Coulombic screening has on energetic ions. At high ion velocities, the probability of ion interaction with electrons is much higher than with nuclei. The electrons effectively "screen" the nuclei from repelling away from the charged particles.

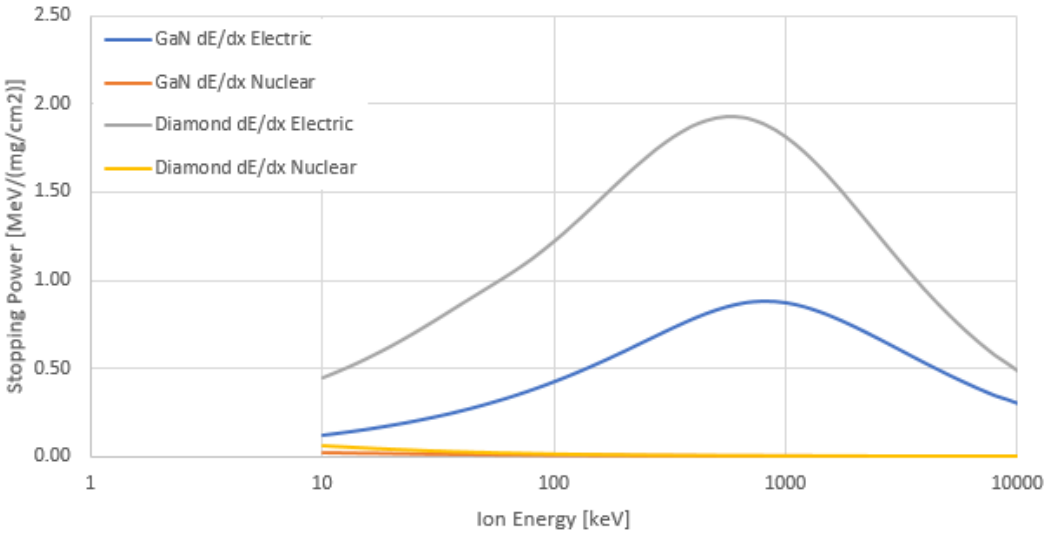

Fig. A-1 Electronic and nuclear stopping vs. ion energy in diamond and gallium nitride (GaN) as calculated in Stopping and Range of Ions in Matter (SRIM)

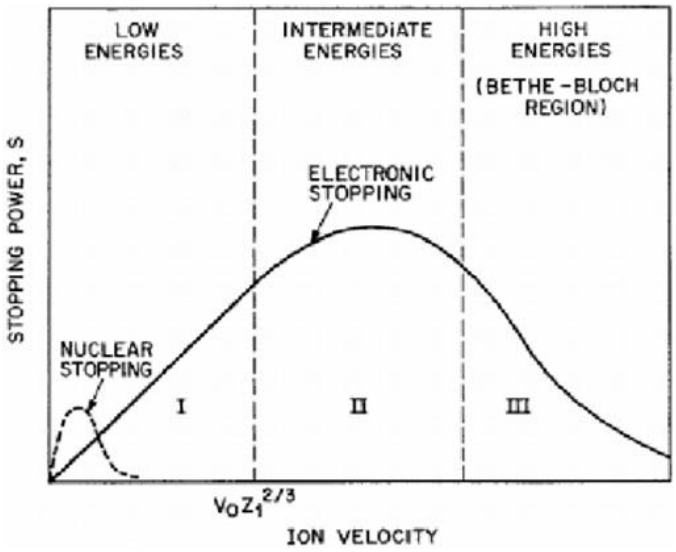

Fig. A-2 Electronic and nuclear stopping probability vs. ion energy

Figure A-3 compares ionization energy deposition in GaN from betas and alphas. Not only do alpha ranges match up well with direct energy converter dimensions, but they provide energy several orders of magnitude higher than alphas.

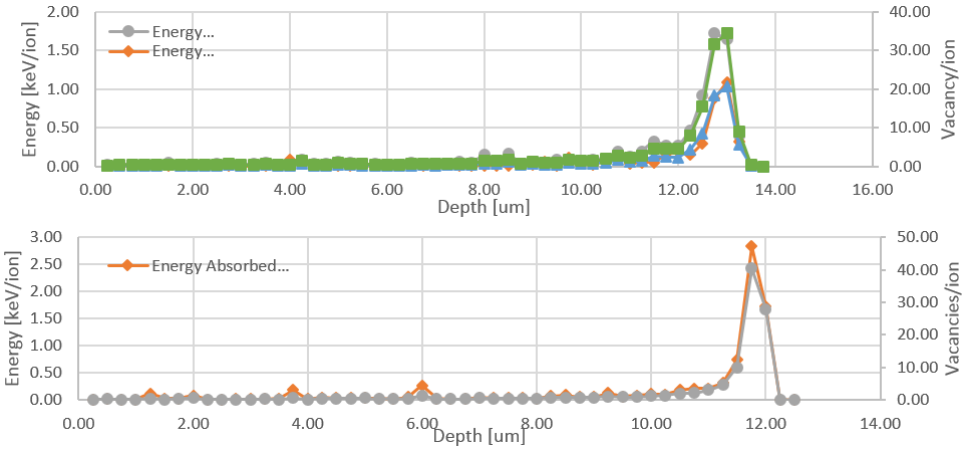

Fig. A-3 Alpha radiation induced vacancies per ion and recoil energy by depth in gallium nitride (top) and diamond (bottom)

Calculation of required ^{241}Am activity for 10 mW/cm^3 power density:

For a 1- × 1-cm^2 device, the output power parameter, P_{out}, is 1 mW. Using this constraint, the required activity, A_{req}, was found. The depletion region and Schottky region of 1-μm width in diamond collect 19% of the total α ionization energy, P_{tot} and have maximum charge collection efficiency of 44.2%.[1] Now, 19% of P_{tot} is P_{out}; P_{tot} = 0.005263 W.

$$P_{tot} = A_{req}\,[Ci] * \frac{3.7*10^{10}\left[\frac{decay}{s}\right]}{1\,[Ci]} * 5\left[\frac{MeV}{decay}\right] * 1.6022 * 10^{-13}\left[\frac{J}{MeV}\right] * 44.2\% = 0.005263. \quad \text{(A-1)}$$

A_{req} = 0. 0.4017 Ci. Thus, 10 1- × 1-cm^2 devices with thickness of 0.1 cm would achieve 10 mW/cm^3 power density with 4 Ci of ^{241}Am.

Prelas worries about Schottky devices[1]:

> The surface interface between the metal and semiconductor forms a depletion region that is effectively 100s of nanometers thick. Thus the effective size of the energy conversion region is thin and not well matched to the ranges of ionizing radiation. The theoretical maximum efficiency for Schottky barrier structures is approximately 0.3% for alphas and approximately 0.1% for low-energy betas. Schottky barriers are less susceptible to radiation damage since the atomic layer bonding the metal to the semiconductor is thin and is thus less prone to displacements caused by the radiation.

[1] Prelas M, Weaver C, Watermann M, Lukosi E, Schott R, Wisniewski D. A review of nuclear batteries. Prog Nucl Energy. 2014;75:117–148.

INTENTIONALLY LEFT BLANK.

Appendix B. Alpha Photovoltaics

Alpha photovoltaics are inherently less efficient than alpha-voltaics approaches because they involve a 2-step energy conversion process. However, instead of only collecting energy in depletion regions the full 50-µm energy deposition generates photons. The optical self-attenuation of zinc sulfide (ZnS) is on the order of 300 µm. Therefore, the entire α energy deposition range in ZnS (approximately 50 µm) would become active conversion volume.

An experiment documenting the radiation effects in ZnS from both ^{241}Am and ^{147}Pm would be useful. The energy deposition from 5-MeV alpha particles is shown in comparison for diamond, gallium nitride (GaN), and ZnS (both crystalline and powder density). The 50-µm α energy deposition in ZnS powder is comparable to the energy deposition of ^{147}Pm in ZnS phosphor powder. Figure B-1 shows that the point at which 50% of the energy is deposited is 7.25 µm in diamond, 7.5 µm in GaN, 10.75 µm in crystalline ZnS, and 29.25 µm in powdered ZnS.

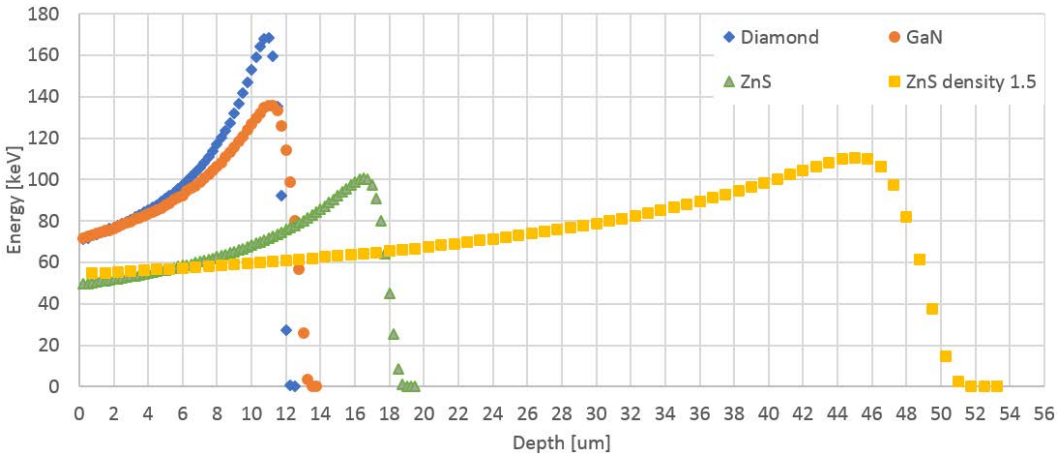

Fig. B-1 Ionization from 5 MeV alpha particles in diamond, GaN, and ZnS (crystalline and powder form)

Stopping and Range of Ions in Matter (SRIM) data was used for alpha energy deposition. Alpha energy curves do not fit well to equations because of the abrupt Bragg peak. Casino MonteCarlo software was used to model energetic electron deposition in diamond, GaN, and ZnS. The equations of the beta energy deposition curves were approximated from curves of best fit. Error in the fit was minimized using sixth-order polynomials.

Equations of Best Fit for Beta Energy Deposition in Diamond, GaN, and ZnS (6th order)

The results of both α and β exposure to diamond are shown in Fig. B-2. The resulting polynomial fits are documented below. Units are x [nm] and y [keV/bin resolution]. The data for 6, 16, and 62 keV betas was binned in 50 rows with lengths of 10, 60, and 400 nm for diamond and GaN, and 30, 100, and 800 nm for ZnS, respectively.

6 keV Diamond

Y = 6.53665734e–15*x6 – 4.65238219e–12*x5 + 1.23441182e–09*x4 – 1.91210138e–07*x3 + 1.55647350e–05*x2 + 5.88740888e–04*x + 1.34077954e–01

16 keV Diamond

Y = 8.96919349e–19*x6 – 4.15533358e–15*x5 + 7.46487794e–12*x4 – 7.13710970e–09*x3 + 3.40791321e–06*x2 – 8.08433353e–05*x + 3.78807896e–01

62 keV Diamond

Y = 1.86927178e–24*x6 – 9.04886259e–20*x5 + 1.68461304e–15*x4 – 1.64399530e–11*x3 + 8.10035963e–08*x2 – 4.00480095e–05*x + 9.16403322e–01

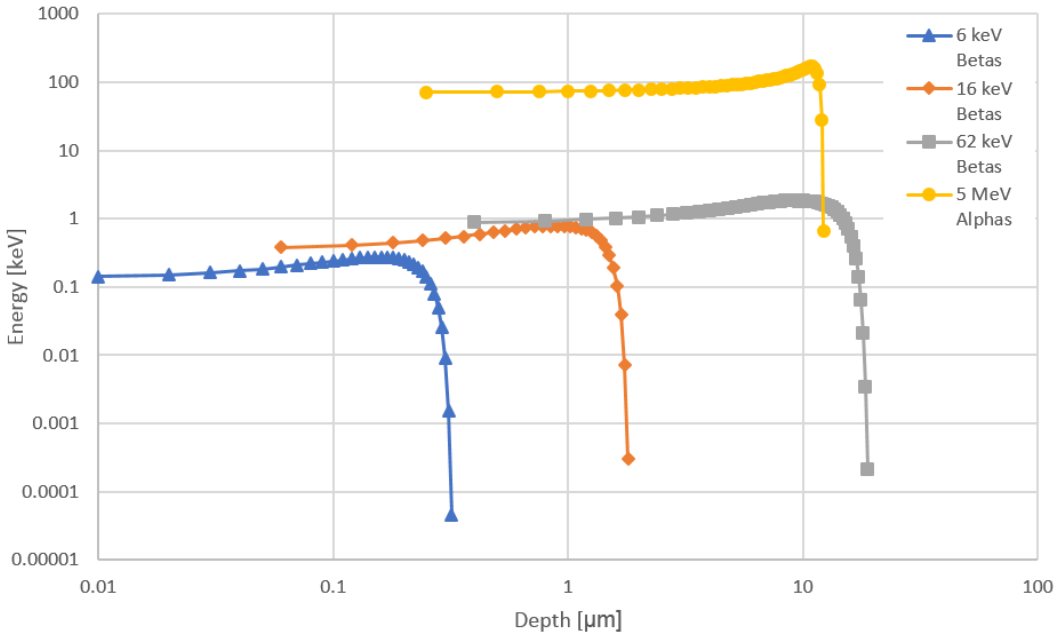

Fig. B-2 Energy deposition in diamond from alphas and betas

The results of both α and β exposure to GaN are shown in Fig. B-3. The resulting polynomial fits are documented as follows:

6 keV GaN

Y = 4.72994855e–15*x6 – 5.22856553e–12*x5 + 1.71652302e–09*x4 – 5.38495442e–08*x3 – 5.65357075e–05*x2 + 5.40988353e–03*x + 2.68898374e–01

16 keV GaN

Y = –1.01586031e–18*x6 + 3.68016766e–15*x5 – 7.39146675e–12*x4 + 1.29819142e–08*x3 – 1.36947046e–05*x2 + 4.75685514e–03*x + 7.90436254e–01

62 keV GaN

Y = –7.95513290e–24*x6 + 3.20772785e–19*x5 – 5.96773805e–15*x4 + 7.33876160e–11*x3 – 5.60818854e–07*x2 + 1.62557425e–03*x + 2.13081118

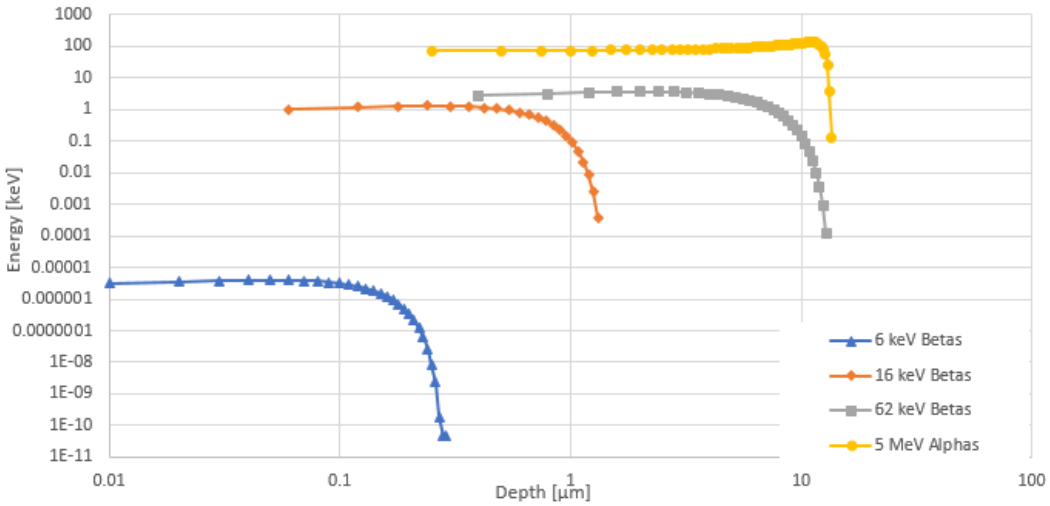

Fig. B-3 Energy deposition in GaN from alphas and betas

The results of both α and β exposure to ZnS are shown in Fig. B-4. The resulting polynomial fits are documented as follows:

6 keV ZnS

$Y = -1.70075884e{-}19*x^6 - 3.79113115e{-}16*x^5 + 5.13216595e{-}13*x^4 + 2.30430430e{-}09*x^3 - 3.57287072e{-}06*x^2 + 1.09656646e{-}03*x + 2.08602288e{-}01$

16 keV ZnS

$Y = -2.63598526e{-}22*x^6 + 4.05783412e{-}18*x^5 - 2.80869319e{-}14*x^4 + 1.34021049e{-}10*x^3 - 4.27129158e{-}07*x^2 + 5.13251918e{-}04*x + 3.51838580e{-}01$

62 keV ZnS

$Y = -7.49152936e{-}28*x^6 + 1.56740887e{-}22*x^5 - 1.29004348e{-}17*x^4 + 6.21145060e{-}13*x^3 - 1.78947376e{-}08*x^2 + 1.96593691e{-}04*x + 1.11933084$

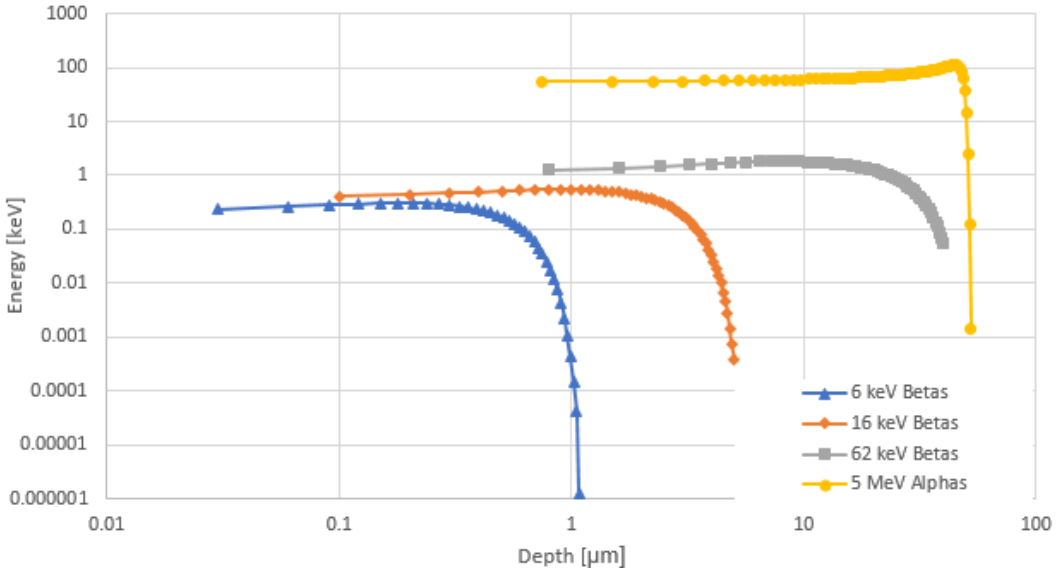

Fig. B-4 Energy deposition in ZnS from alphas and betas

*The file for alpha radiation deposition is listed as "Alpha Ionization in diamond, GaN, and ZnS SRIM.xlsx".

INTENTIONALLY LEFT BLANK.

List of Symbols, Abbreviations, and Acronyms

ARL	US Army Research Laboratory
BPV	beta photovoltaic
CCE	charge collection efficiency
DARPA	Defense Advanced Research Projects Agency
E_0	energy imparted
E_d	lattice displacement energy
EHP	electron-hole pair
GaA	gallium arsenide
GaN	gallium nitride
LET	linear energy transfer
MSU	Michigan State University
NIEL	nonionizing energy loss
SBD	Schottky barrier diode
SRIM	Stopping and Range of Ions in Matter
ZnS	zinc sulfide

1 (PDF) DEFENSE TECHNICAL INFORMATION CTR DTIC OCA

2 (PDF) DIR ARL
RDRL DCM
IMAL HRA RECORDS MGMT
RDRL DCL
TECH LIB

1 (PDF) GOVT PRINTG OFC
A MALHOTRA

4 (PDF) DIR ARL
RDRL SED E
J LANGLEY
M LITZ
J RUSSO
W RAY